A finite element method for 1D and 2D shallow water

J.M[a]. Emperador & B. Hernandez
Department of Civil Engineering, Las Palmas de Gran Canaria University, Campus de Tafira s/n 35094 Canary Islands, Spain
Email: emperado@fobos.ulpgc.es, bhernan@iac.es

Abstract

The finite element method has been used to develop two numerical tools for a Boussinesq shallow water equation, 2DH and 1DH. In both models, an automatic unstructured mesh generator has been employed to assure the convergence and stability of the numerical solution through the assumption of a Courant number close to one in the whole domain. Partially reflecting- absorbing boundary conditions has been carried out to model the open seaward contour and other contour types. In the 1DH numerical model has been carried out the finite element version of the Deigaard et al break wave model and it is valid for spilling breaks. A new intuitive and numerical break rule has been developed to simulate the plunging break mode. The results obtained with both models had been compared with the equivalent results of others numerical methods and experimental data for the same problem type such as pure diffraction and step varying bottoms.

1 Introduction

1.1 Shallow water models

In the last years an important effort has been done to develop numerical tools that allows us to model and analyze the sea wave propagation properly. The main theoretical models used are based on the reduction at least of one dimension of the problem through the vertically integrated velocity assumption, 2Dh models. In this paper the Boussinesq [1] model is selected By taking into account the vertical acceleration, this model allows us to model correctly the behavior of the wave in shallow water until the nearness of the break point.

1.2 Break models

In this paper an extension of the Boussinesq model after the break point of the wave is supposed. The most break models used are based on wave parameters and are associated with energy dissipation.

Another effort has been done by Tao [2], Abbot et al [3], Karambas & Koutikas [4] to extend the Boussinesq model up to the break zone, on this case the energy dissipation is associated to an additional eddy viscosity term.

Deigaard [5] has made an approach based on similar ideas to the model for the hydraulic jump of Engelund [6] and has used the surface roller concept. In this model the breaking process begins when the local slope of the wave front reaches a certain value. The model is only valid for the spilling break mode. For other break modes turbulent models are established. In this paper, a numerical and intuitive rule has been introduced and where the amplitude and local velocity of the wave have been affected by coefficients that reduce its values.

2. Govern equations

The governing equation is the Boussinesq. The form used is the simplest. The mass and linear moment, in x and y co-ordinates, conservation equations are:

$$\dot{\eta} + \left[(h+\eta)\cdot U\right]_{,x} + \left[(h+\eta)\cdot U\right]_{,y} = 0$$

$$\dot{U} + U\cdot U_{,x} + V\cdot V_{,y} + g\cdot\eta_{,x} = h^2/3\cdot\left[\dot{U}_{,xx} + \dot{V}_{,xy}\right] \qquad (1)$$

$$\dot{V} + U\cdot V_{,x} + V\cdot U_{,y} + g\cdot\eta_{,y} = h^2/3\cdot\left[\dot{U}_{,xy} + \dot{V}_{,yy}\right]$$

Where h is the mean water level deep, η is the amplitude over the MWL,and U & V are the vertically integrated horizontal velocities. In these equations do not include the viscosity, bottom friction and wind effects term.

2.1 Break models

In the paper, we have carried out a 1DH finite element version of the surface roller model and developed a numerical rule for plunging breaks.

Many break criteria exist and the most useful are those based on the local parameters such as:$\eta b/Hb=r$,wave height to deep at break point and the critical wave front slope, tan φbr.

2.2.1 Surface roller model

This model developed by Deigaard et al [5] is based on the consideration of two zones; the first one water with ondulatory movement and the second one as a roller of air and water travelling with the wave celerity over the water surface. The roller geometry is shown in Figure 1.0, where δ is the roller thickness.

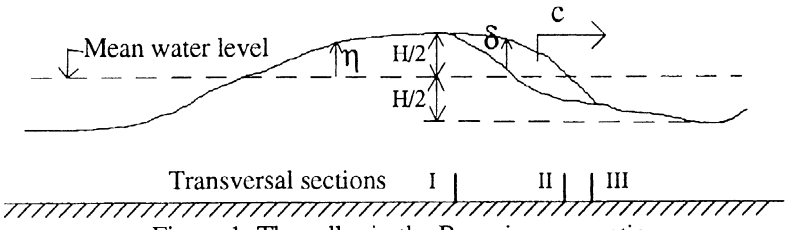

Figure.1: The roller in the Boussinesq equation

The 1DH model expression of the additional pressure term that modifies the dynamic and ondulatory movement, simulating the interaction between the wave and the roller extracting the energy,.is .

$$dP = -\rho g(\delta \cdot h_{,x} + (h+\eta)\cdot \delta_{,x})\cdot dx \qquad (2)$$

The roller geometry is determined experimentally by Deigaard using φbr= 27°as initial break angle and φbr= 10° as the break cessation value.

2.2.2 Coefficient rule

The coefficient rule has been established as to multiply the wave amplitude and the local velocity by the factors, $K\eta$ & KU respectively that allow us to simulate the abrupt loss of energy in the plunging break mode. The rule is purely numerical and it will be mentioned in the appropiate paragraph.

3. Numerical 2DH model

A finite element technique is used to obtain a governing equations numerical model. A standard Galerkin of weak solution with $\phi\alpha$ ponderation function, $\phi\beta$ and $\phi\gamma$ functions for variables and bathymetric aproximation respectively, isoparametric triangular and quadrilateral element is obtained with this procedure for the spatial discretization. The temporal discretization is based on predictor -corrector procedure. The method used is based on Kawahara et al [7] and includes a lumped parameter in the mass matrix.

The elemental integral of the products of the aproximation function and their spatial derivatives is given by the convention:

$$X_{\alpha x \beta y \gamma x} U_\beta V_\gamma = \int_\Omega \Phi_{\alpha,x} \cdot \Phi_{\beta,y} \cdot \Phi_{\gamma,x} \cdot U_\beta V_\gamma \cdot d\Omega e \qquad (3)$$

The governing equations can be expressed now by:

$$M_{\alpha\beta}\cdot\dot{\eta}_{\beta}+N_{\alpha\beta x\gamma}\cdot U_{\beta}H_{\gamma}+L_{\alpha\beta\gamma x}\cdot U_{\beta}H_{\gamma}+J_{\alpha\beta y\gamma}\cdot V_{\beta}H_{\gamma}+I_{\alpha\beta\gamma y}\cdot V_{\beta}H_{\gamma}=0$$

$$\left[M_{\alpha\beta}+\frac{h^2}{3}\cdot\left(K_{\alpha x\beta x}+G_{\alpha x\beta y}\right)\right]\cdot\dot{U}_{\beta}-\frac{h^2}{3}\cdot C_{\alpha\beta x}\cdot\left(\dot{U}_{\beta}n_1+\dot{V}_{\beta}n_2\right)+ L_{\alpha\beta\gamma x}U_{\beta}U_{\gamma}+I_{\alpha\beta\gamma y}V_{\beta}U_{\gamma}+A_{\alpha\beta x}\cdot\eta_{\beta}=0 \quad (4)$$

$$\left[M_{\alpha\beta}+\frac{h^2}{3}\cdot\left(P_{\alpha y\beta y}+Q_{\alpha y\beta x}\right)\right]\cdot\dot{V}_{\beta}-\frac{h^2}{3}\cdot D_{\alpha\beta y}\cdot\left(\dot{U}_{\beta}n_1+\dot{V}_{\beta}n_2\right)+ L_{\alpha\beta\gamma y}V_{\beta}V_{\gamma}+I_{\alpha\beta\gamma x}U_{\beta}V_{\gamma}+Z_{\alpha\beta y}\cdot\eta_{\beta}=0$$

Briefly:

$$M\dot{\hat{\eta}}=f(\hat{U},\hat{V},\hat{H});MKG\dot{\hat{U}}=g(\hat{U},\hat{V},\hat{\eta});MPQ\dot{\hat{V}}=h(\hat{U},\hat{V},\hat{\eta}) \quad (5)$$

3.1 Temporal discretization

The temporal schema obtained is implicit and linear between two sucessive iterations. The weighed residual method is used to obtain the temporal formulation, which at first uses different Wi weighting functions for the wave height and velocity. Depending on the selected function different temporal schemata were obtained:

$$\hat{x}=\alpha\cdot\hat{x}^{k+1}+(1-\alpha)\cdot\hat{x}^{k} \qquad \text{and} \qquad \dot{\hat{x}}^{k+\alpha}=\left(\hat{x}^{k+1}-\hat{x}^{k}\right)/\Delta t \quad (6)$$

where x represents one of the variables η, U and V. Introducing this schemata in the equation (5) it can be obtained the following:

$$\begin{aligned}&\tilde{M}\hat{\eta}^{k+1}=\overline{M}\hat{\eta}^{k}+\Delta t\cdot f(\hat{U}^{k+\theta},\hat{V}^{k+\theta},\hat{\eta}^{k+\alpha})=0\\&MKG\hat{U}^{k+1}=MKG\hat{U}^{k}+\Delta t\cdot g(\hat{U}^{k+\theta},\hat{V}^{k+\theta},\hat{\eta}^{k+\alpha})\\&MPQ\hat{V}^{k+1}=MPQ\hat{V}^{k}+\Delta t\cdot h(\hat{U}^{k+\theta},\hat{V}^{k+\theta},\hat{\eta}^{k+\alpha})\end{aligned} \quad (7)$$

where $\tilde{M}$ and $\overline{M}$ are the lumped and mixed mass matrices. They are related to the **e** lumped parameter of Kawahara et al [7], by the following expression:

$$\overline{M}=e\cdot\tilde{M}+(1-e)\cdot M \quad (8)$$

The suggested value of the lumped parameter is: $0.8\le e\le 1.0$ and it is object of further discussion

3.2 Boundary Conditions

If the problem is correctly formulated the boundary condition will verify the present boundary condition. The main thing is that this condition must not

introduce artificial seaward reflection in an open boundary. In general, the next expressions are frequently used:

$$\eta_T = \eta_I + \eta_S \qquad \underset{\sim}{U}_T = \underset{\sim}{U}_I + \underset{\sim}{U}_S \qquad \underset{\sim}{U}_T = (1-\gamma)\cdot\frac{c\cdot\eta}{h+\eta}\cdot\underset{\sim}{u} \qquad c = \sqrt{g\cdot h} \tag{9}$$

where γ is the reflection coeficient. Imposing no normal velocity and in the continuity equation the elevation as unknown at the boundary [8]. The continuity equation at the boundary is:

$$\tilde{M}\eta_s^{k+1} = \overline{M}\cdot(\eta_T^k - \eta_I^k) + \Delta t\cdot f(U_T^{k+\theta}, V_T^{k+\theta}, \eta_T^{k+\alpha}) = 0 \tag{10}$$

The first condition results, as in the governing equation with the same procedure, in the set of equation one on each direction, x and y.

$$\begin{aligned} A_{\alpha\beta x}\cdot ux_{T\beta} + Z_{\alpha\beta y}\cdot ux_{T\beta} &= 0 \\ A_{\alpha\beta x}\cdot uy_{T\beta} + Z_{\alpha\beta y}\cdot uy_{T\beta} &= 0 \end{aligned} \tag{11}$$

This set of equations is only solved for the boundary nodes.

3.3 Numerical 1DH and break models

When the domain characteristics are constant in the transversal direction the whole model can be simplified to one dimension, neglecting the variables and its derivatives. When the surface roller model of breaking is carried out from equation(3) as such in Bossinesq equation the results are given by:

$$M_{\alpha\beta}\cdot\dot{\eta}_\beta + N_{\alpha\beta\gamma}\cdot U_\beta H_\gamma + L_{\alpha\beta\gamma}\cdot U_\beta H_\gamma = 0 \tag{12}$$

$$\left(M_{\alpha\beta} + \frac{h^2}{3}\cdot K_{\alpha\beta x}\right)\cdot\dot{U}_\beta + L_{\alpha\beta\gamma}U_\beta U_\gamma + g\cdot\left[A_{\alpha\beta x}\cdot\eta_\beta + k_r\cdot L_{\alpha\beta\gamma x}\cdot(\delta_\beta\eta_\gamma + H_\beta\delta\gamma)\right] = 0$$

3.4 Parametric analysis of the model

The model has been built with three parameters, α, θ and **e.** An example of parametric analysis has been done. This example consist in 1 m height solitary wave in a channel of uniform depth .

3.4.1 Temporal discretization parameters α yθ

Several values of both parameters have been used in the analysis. The results are given in Figure 2 when both have the same value. It can be seen that the values of 0.5 is the only one that performs a stable and correct artificial diffusivity in the model

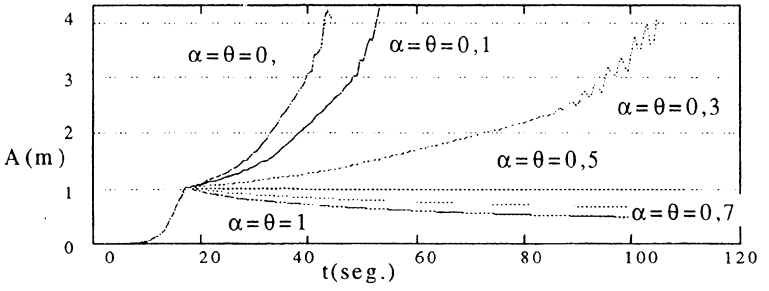

Figure2: Amplitude (max.elevation) vs time for different $\alpha=\theta$ values

3.4.2 Lumped mass matrix parameter

When the same channel is used with a 1 m heigth sinusoidal wave train it can be seen that the numerical procedure shows a wave height decrease and this is bigger with the channel lenght. In Figure 3 it can be compare several values of the lumped mass matrix parameter. It introduces artificial diffusivity in the model which is greater as when closing to the lowest suggested value. The figure shows that the 1DH finite element method obtains a lower height decrease than the finite differences method when the parameter is equal to one and all the methods show an important wave height decrease when the channel is very long. In the usual flume channel length all the values of the parameter are close and does not shows significant differences.

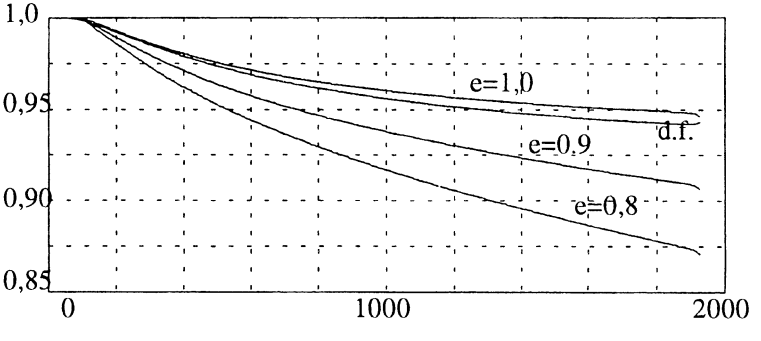

Figure 3: Wave height decrease vs **e** parameter

For all of these analysis the values adopted are $\alpha=\theta=0.5$ and e=1.0 for 1DH model and 0.9 for 2DH model.

3.5 Unstructured mesh

To assure the correct convergency and numerical stability, it is necessary that the value of the Courant number be close to one in the whole domain. This leads to obtain an unstructured mesh with an unequally spaced nodes and it is

adapted to the bathymetry with a minimum of nodes over a wave lenght, usually 10.

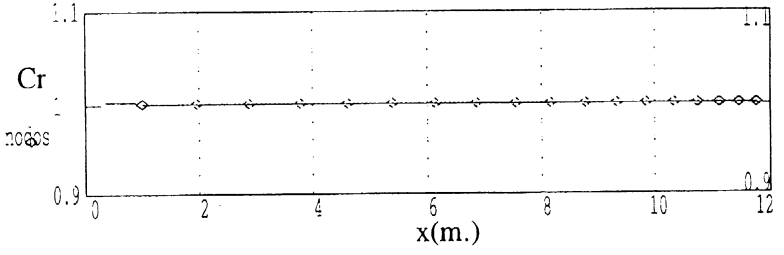

Figure 4: Nodal distribution and Cr variation

In this case the technique consist in obtaining the new nodal co-ordinate of the next node from:

$$x_i = x_a + \sqrt{g \cdot h_a}/K \text{ and } K = 1/\Delta t$$

Figure 4 show the nodal distribution and the Courant value of those for one example of constant slope bed from (0.0,-4.0 to 12.0,0.0).

3.5.1 2DH Mesh

In two dimensional domains this technique is extrapolated but the difficulties are greater [9,10] In the paper, an unstructured automatic mesh generator for triangular elementswas developed. The procedure is based on the generation of internal and boundary nodes that comply with the C.F.L. condition from points with known bathymetry through the frontal advance technique [10,11]. In Figure 5 we can see the gererated mesh and the same after that the smoothing technique is used to obtain elements with a better aspect ratio.

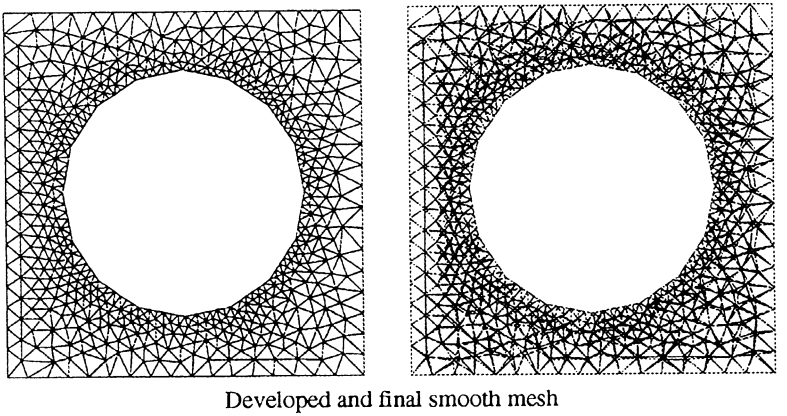

Developed and final smooth mesh

Figure 5: Unstructured triangular mesh obtained from frontal method

4.0 Solution Algorithm

The solution algorithm used is:

1) Obtain the values of η,U,V from the previous or initial time step.

2) Obtain the value of η for the instant $t+\Delta t$ at the k+1 iteration from the continuity equation and the previous values.

3) Obtain the scattered values of the wave variables, η,U,V, at the boundary

4) Obtain the elevation η at $t+\alpha\Delta t$ from k+1 and k iterations

5) Obtain the U,V values at $t+\Delta t$ in the k+1 iteration from the momentum equations and the values from steps 2 and 3.

6) Obtain the scattered wave direction from the set of equations (11)

7) Obtain the Uy V at $t+\theta\Delta t$ from k+1 y k iterations

8) Obtain the value of η at $t+\Delta t$ in k+1 iteratiopn from the continuity equation and the results of the steps 3 and 5

9) Return to 4 step and repeat through the 8 except for step 6 up to:

$$\sum_{i=1}^{nnode} \sqrt{\left(\hat{\eta}_i^{n} - \hat{\eta}_i^{n-1}\right)^2 / \eta_{max}^2} < Tol$$

10) Begin the next iteration.

In all the process it was necessary to solve two systems of linear algebraic equations. The first in η and the other in U,V. All of those are sparse and it is essential to use a Solver Library for large and sparse systems of equations. The library used is the Meschach.

5.0 Numerical Results

5.1 1DH results and break model

The example to be solve consists of a 1:30 constant slope, from -3.0 to -0.1 m deep and 90 m length, beach.. The input is a solitary wave with 0.5 m height. The next sections show the results obtained from the implemented break model and for the developed coefficients rule.

5.1.1 Surface roller model results

The roller model parameter is the usual found in the literature and its values are: Angular break criteria: tan φb=0.33, lowest roller slope: tan φo=0.173 and roller form factor kr=1.5

Figure 6 show the wave height versus time. In the zone I the wave comes into the domain up to its nominal height. The zone II, shows the shoalling effects of the variable bed and the wave heihgt increases up to begining of the break. The zoneIII, shows the evolution during the roller action, the decrease

in height is aproximately lineal in time. This is the spilling break mode. The zone IV,shows the beginnig of a new shoal and finally in, V, a new break.

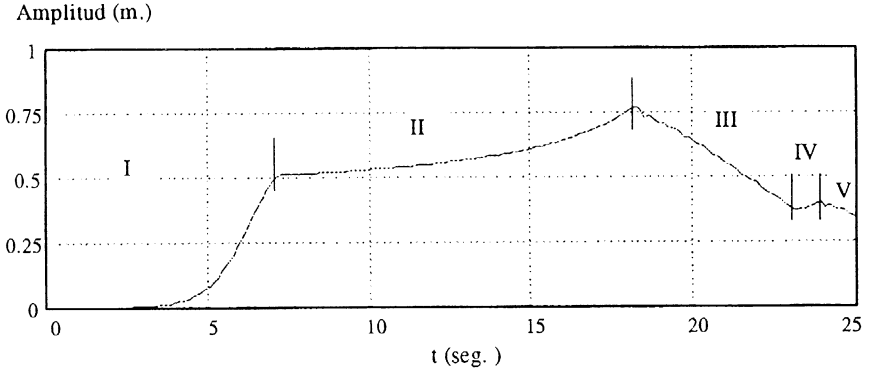

Figure 6: Spilling break, crest point position versus time

5.1.2 Reduction coefficient rule

In this rule the break model parameter are: $\eta b/hb=0.8$ and $k\eta=0.5$, $kU=0.1$ The velocity are sharply reduced and the wave height reduction is limited to the 50% [12].

Figure 7 shows that the zones I and II are similar to Figure 6. In the zone III the wave height decrease is abrupt, plunging break. The IV zone shows a new shoal and in the V zone the wave shows a new abrupt break. The distance between the first and second break is shorter than in the roller model.

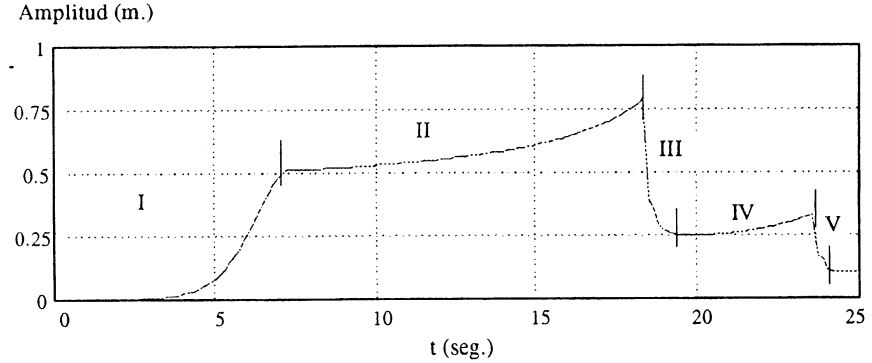

Figure 7: Coefficient rule 0.5/0.1, crest point position versus time

In the next case the same rule was used. The only change takes place in the reduction coefficient values: $k\eta=0.7$ and $kU=0.9$, 30% in height decrease and 10% in velocity.

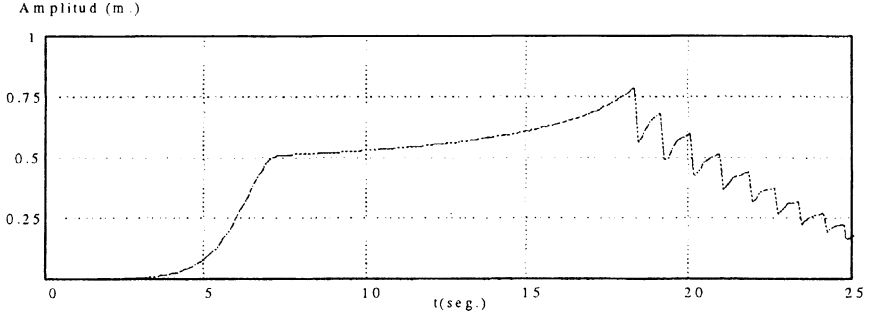

Figure 8: Coefficient rule 0.7/0.9, crest point position versus time

Figure 8 shows that the wave have several and successive break with a progressive height decrease, practically lineal in time. It shows that this model converges over the roller model when the celerity of the wave is the initial and the reduction in height is small.

The rule presented in this paper needs to calibrate the factor reduction values from experimetal test for several bed slopes and Iribarren parameters.

5.1.3 Step bed channel

This section shows the results of a step bed channel and it is compared with those experimental data obtained from phisical model from the Institute de Mecanique de Grenoble. The geometry of the channel and the four wave-gauge position are shown in Figure 9.

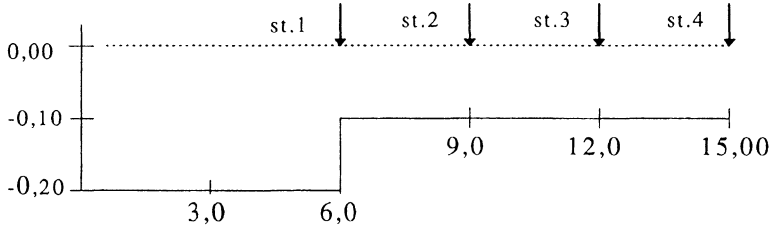

Figure 9: Geometry channel and wave gauge position

Figure 10 shows the results for the following excitation data: wave amplitude, A=0.0365 m.

The computed results show a good agreement in amplitude and phase with the measured data and with the numerical results of Antunes do Carmo et al [13]:

	Present	Reference	Experimental
First transmitted wave,	A1=0.0560 m	0.0560 m	0.0531 m
Second Transmitted wave,	A2=0.0197 m	0.0240 m	0.0180 m
Third transmitted wave,	A3=0.00321m	0.0040 m	0.0033 m

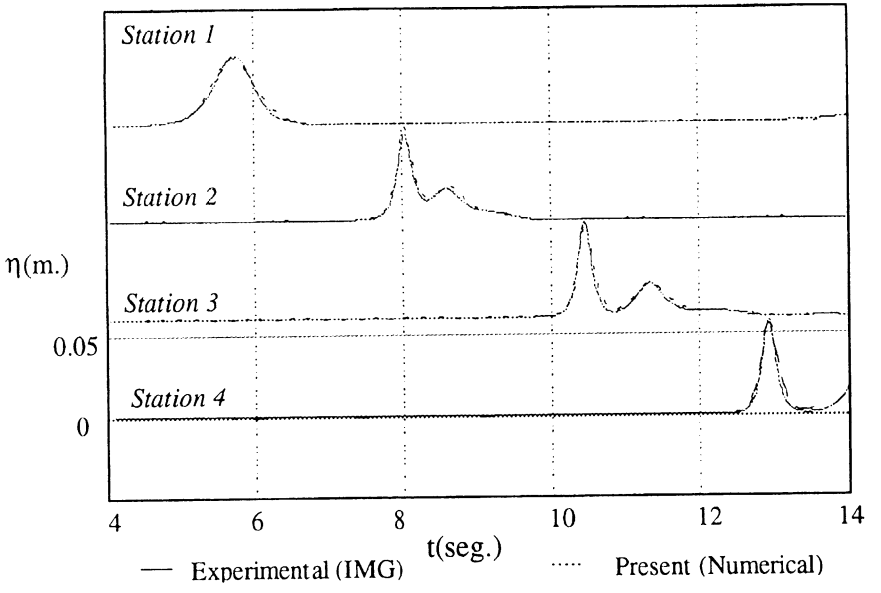

Figure 10 : Numerical and experimental comparation

5.2 2DH model results

This section shows the results in the case where the two-dimensional domain discretization is absolutely needed. Two examples of this case are shown. The first one is a channel with a vertical cilinder island as in the reference and the other is a detached breakwater.

5.2.1 Channel with island

Figures 11 and 12 show the plan view of the channel of 0.15 m. deep and the unstructured mesh, respectively, with 1505 nodes and 2788 triangular elements. The Courant number is close to one in the whole domain. The solitary wave amplitude is A=0.0375 m.

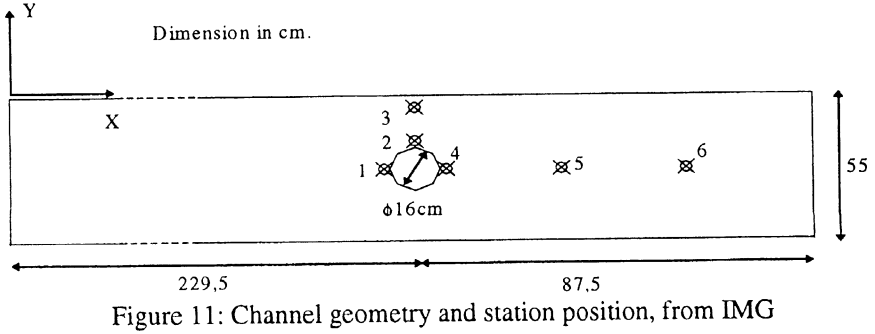

Figure 11: Channel geometry and station position, from IMG

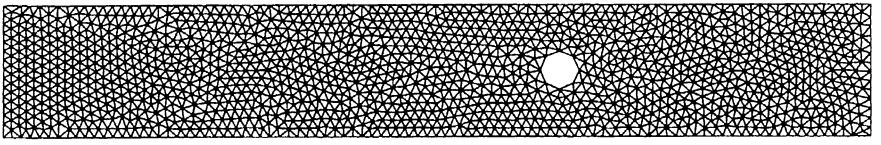

Figure 12: Finite element mesh

In Figure 13 we can see the comparation of the present results with those of the reference [13] and the experimental data in the six measured stations.

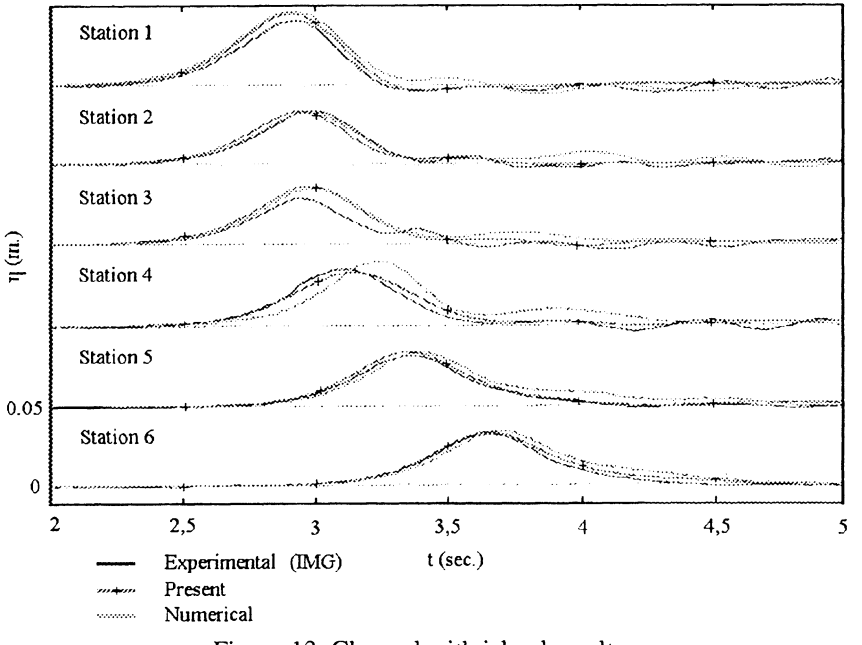

Figure 13: Channel with island results.

The results of the present method show a good agreement, in amplitude with the experimental data in all the stations except for the number 3 where the experimental is lowest of the results obtained from both numerical methods . The agreement in the fourth station, in amplitude and in phase between the present method and measured data is good and with a sligthly better aproximation in phase than the other numerical method [13].

5.2.2 Detached breakwater

This example shows both the qualitative aspects of the model and the correct formulation of the boundary conditions with absorbing and reflecting boundary

The parameters of the model are:

Boundary	Wave condition	B. Condition
Left	A=1. m, λ_0=150	-
Bar walls		γ=1.0
Lateral walls		γ=1.0
Right		γ=0.0

Figure 14 shows the situation when the simulation time lasts 60 seconds. It can be seen that several wave which are into the inner zone are diffracted and the form of the outer reflected wave [11].

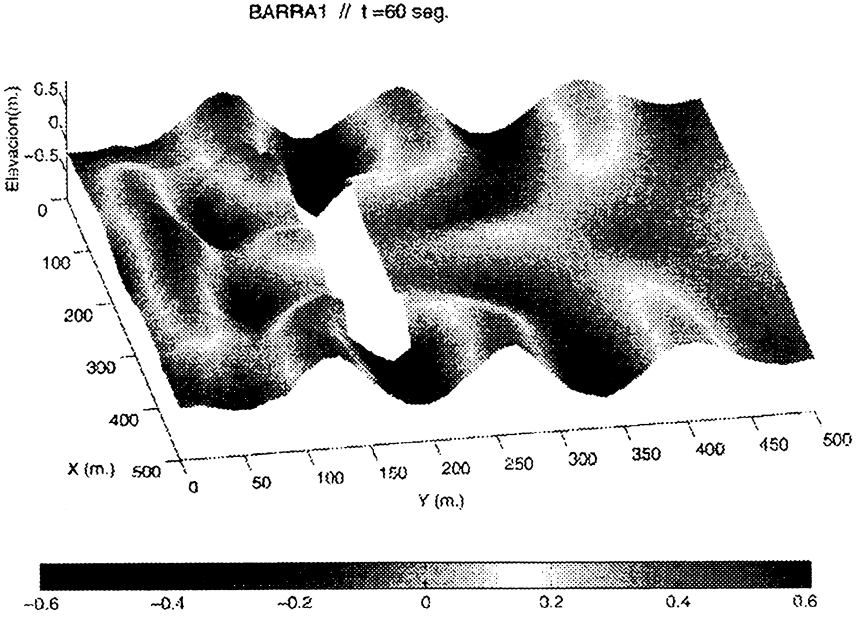

Figure 14: Water surface at 60 seconds of simulation.

6.0 Conclusions

The developed finite element model in both 1DH and 2DH versions allows the simulation of wave propagation over shallow water and for any kind of geometry and with several boundary conditions which include the reflecting and absorbing ones. This method togeter with the automatic unstructured mesh generator developed improve the accuracy and the stability of the numerical procedure.

In the one dimensional model, one break model and a rule have been caaried out. The first is the finite element version of the previous finite difference and it show a good behavior with variable bottoms geometry. The coefficient rule

work well numericaly for solitary waves. However, it must be experimentally tested to obtain the correlation between its values and the local break criteria.

The time solution algorithm used allows us introduce an abrupt perturbation without any loss of stability and accuracy in the model as the above procedure perform.

Acknowledgements

The authors greatfully acknowledgement to the Canary Astrophysical Institute, for the facility in the use of its computational media, in the develop of this work as well as to the University of Las Palmas of Gran Canaria for the support and to the authors of the Meschach Library for the use of their sparse matrix solvers library

7.0 References

1. Boussinesq, J. `Théorie des ondes et des remous qui se propagent le long d´un canal rectangulaire horizontal, L. Math. Pure et Appl., 2(17),55-108, 1872.
2. Tao, J. `Computation of Wave Runup and Wave Breaking´, Internal Report , Danish Hydraulic Institute,Hosholm, 1983
3. Abbott, M.B., Larsen, J., Madsen, P. & Tao, J. Simulation of Wave Breaking and Runup in Seminar an Hydrodinamics of Waves in Coastal areas, Arr. by IHAR in conection with the 20th Congress of IHAR, Moscow, 1983
4. Karambas, Th. & Koutikas, C. A Breaking Wave Propagation Model based on Boussinesq Equations, Coastal Engineering, Vol. 18, pp 72-20, 1992
5. Deigaard, R. Mathematic modeling of Waves in the Surf Zone ,Progres Report 69, pp 47-59, ISVA, Thecnical Univ. Lingby, Denmark, 1983.
6. Engelund, F. A Simple Theory of Weak Hydraulic Jumps, Progress Report 69, pp 29-32, ISVA, 1983
7. Kawahara, M., Hirano, H., Tubota, K. & Inagaki, K. Selective lumping Finite Element Method for Shallow Water Flow, Int. Jour. Num. Meth. in Fluids, Vol. 2, pp 89-112, 1982
8. Sanchez Arcilla, A, Monsó, J.L., Sierra, J.P. Modelo numérico no lineal de ondas de superficie libre, Dirección General de Puertos y Costas, Pub. N° 17 MOPU, 1986
9. Kashimaya, K. & Okada, T., Automatic Mesh Generation Method for Shallow Water Flow Analysis, Int. J. Num. Meth. in Fluids, Vol. 15, pp 1037-1057, 1992
10 Bugeda, G. Utilización de técnicas de estimación de error y generación automática de mallas en procesos de optimización estructural, Tesis Doctoral, E.T.S.I.C.C.y P., Universidad de Cataluña, 1992
11. Hernandez, B. Un modelo de elementos finitos para el estudio hidrodinámico del oleaje, Proyecto Fin de Carrera, E.T.S.I.I. de Las Palmas, U.L.P.G.C., 1995
12.- Peregrine, D.H. Breaking Waves on Beaches, Ann. Rev. in Fluids Mechanics. 15, 149-78, 1983.
13. Antunes do Carmo, J.S., Seabra Santos, F.J. & Barthélemy, E., Surface Waves Propagation in Shallow Waters: A Finite Element Model, Int. J. Numer. Meth. in Fluids, Vol. 16, pp 447-459, 1993.